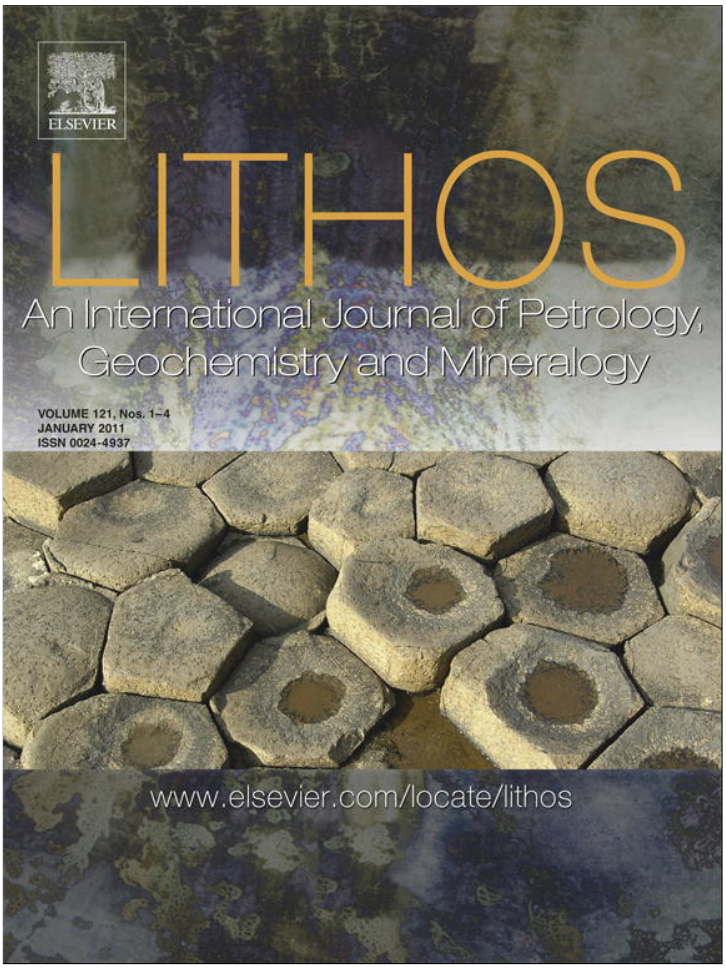

(This is a sample cover image for this issue. The actual cover is not yet available at this time.)

Lithos 134-135 (2012) 41–51

Contents lists available at SciVerse ScienceDirect

Lithos

journal homepage: www.elsevier.com/locate/lithos

Subduction-induced mantle heterogeneity beneath Eastern Tianshan and Beishan: Insights from Nd–Sr–Hf–O isotopic mapping of Late Paleozoic mafic–ultramafic complexes

Ben-Xun Su [a,b,*], Ke-Zhang Qin [a], He Sun [a], Dong-Mei Tang [a], Patrick Asamoah Sakyi [c], Zhu-Yin Chu [b], Ping-Ping Liu [d], Qing-Hua Xiao [a]

[a] Key Laboratory of Mineral Resources, Institute of Geology and Geophysics, Chinese Academy of Sciences, P.O. Box 9825, Beijing 100029, China
[b] State Key Laboratory of Lithospheric Evolution, Institute of Geology and Geophysics, Chinese Academy of Sciences, P.O. Box 9825, Beijing 100029, China
[c] Department of Earth Science, University of Ghana, P.O. Box LG 58, Legon-Accra, Ghana
[d] Department of Earth Sciences, the University of Hong Kong, Pokfulam Road, Hong Kong, China

ARTICLE INFO

Article history:
Received 4 September 2011
Accepted 17 December 2011
Available online 27 December 2011

Keywords:
Central Asian Orogenic Belt
Mafic–ultramafic complex
Mantle heterogeneity
Nd–Sr–Hf–O isotopes
Subduction

ABSTRACT

Extensive late Paleozoic mafic–ultramafic complexes in the Eastern Tianshan and Beishan regions in the southern Central Asian Orogenic Belt (CAOB) represent an ideal opportunity to assess the characteristics of the mantle in this area. Whole-rock Nd–Sr and zircon Hf–O isotopic data from the mafic–ultramafic complexes of the Jueluotage Belt, Middle Tianshan Massif and Beishan Rift were compiled for isotopic mapping. $\varepsilon_{Nd}(t)$ and $(^{87}Sr/^{86}Sr)_i$ values range from +5.5 to +9.5 and 0.702 to 0.706 respectively in the Jueluotage Belt, and from −2 to +11 and 0.703 to 0.710 respectively in the Middle Tianshan and Beishan. Zircon $\varepsilon_{Hf}(t)$ and $\delta^{18}O$ values are in the range of +6.0–+17.0 and 4.14‰–8.00‰ respectively in the Jueluotage Belt, +1–+8 and 5.17‰–6.30‰ respectively in the Middle Tianshan, and show large variations of −1–+17 and 4‰–12‰ respectively in the Beishan. Spatially, the $(^{87}Sr/^{86}Sr)_i$ ratios of mafic–ultramafic complexes increase from the Jueluotage Belt and Beishan to the Middle Tianshan, while the $\varepsilon_{Nd}(t)$ values show an opposite trend and reflect a mixing character between depleted mantle and EM-II reservoirs. Zircon $\varepsilon_{Hf}(t)$ and $\delta^{18}O$ values exhibit an apparent southward decreasing and increasing trends respectively, from the Jueluotage Belt, through Middle Tianshan, to Beishan Rift. Their corresponding Hf model ages increase continuously from north to south. These observations demonstrate that the mantle sources beneath the Eastern Tianshan and Beishan are compositionally heterogeneous, which presumably result from significant and variable degrees of subduction-related modification. We therefore suggest that the late Paleozoic subcontinental lithospheric mantle beneath the Jueluotage Belt was modified by slab-derived melts and fluids during the subduction of the Junggar Ocean, whereas the mantle beneath the Beishan Rift was influenced mainly by slab-derived fluids during the subduction of the South Tianshan Ocean. The unique similarities of the Middle Tianshan mafic–ultramafic complexes reflect a two-stage modification of their mantle source, namely the sequential subduction of the early South Tianshan Ocean, followed by subduction of the Junggar Ocean. Thus, the subduction-induced mantle heterogeneity beneath the CAOB is probably regional in scope.

1. Introduction

The Central Asian Orogenic Belt (CAOB) is the largest Phanerozoic orogen in the world, extending 7000 km E–W, and has a complex evolutional history represented by multi-stage subduction and juvenile crustal growth (Fig. 1A; e.g., Sengör et al., 1993; Hu et al., 2000; Jahn et al., 2000a, b; Hong et al., 2001; Windley et al., 2007; Xiao et al., 2009). The Paleo-Asian ocean has several oceanic arms such as the South Tianshan Ocean and Junggar Ocean, which have subducted under several microcontinents from Proterozoic to Late Paleozoic (e.g., Gao et al., 2009; Su et al., 2011a, b; Sun et al., 2008; Windley et al., 2007; Xiao et al., 2004a). Consequently the lithospheric mantle beneath the CAOB may have been contaminated or modified by subducted crustal materials (e.g., Wang et al., 2009a, 2009b; Zhou et al., 2004). The presence of voluminous juvenile crust in the CAOB implies that a significant amount of mantle material has been extracted from the mantle (Hong et al., 2001; Jahn et al., 2000a, 2004; Su et al., 2011a; Wang et al., 2009a). The significant compositional changes of the mantle may provide essential information on the subduction and melt extraction processes, and may shed more light on the evolution of the CAOB.

* Corresponding author at: P.O. Box 9825, Beijing 100029, China. Tel.: +86 10 82998514; fax: +86 10 62010846.
E-mail addresses: subenxun@mail.igcas.ac.cn (B.-X. Su), kzq@mail.igcas.ac.cn (K.-Z. Qin).

0024-4937/$ – see front matter © 2011 Elsevier B.V. All rights reserved.
doi:10.1016/j.lithos.2011.12.011

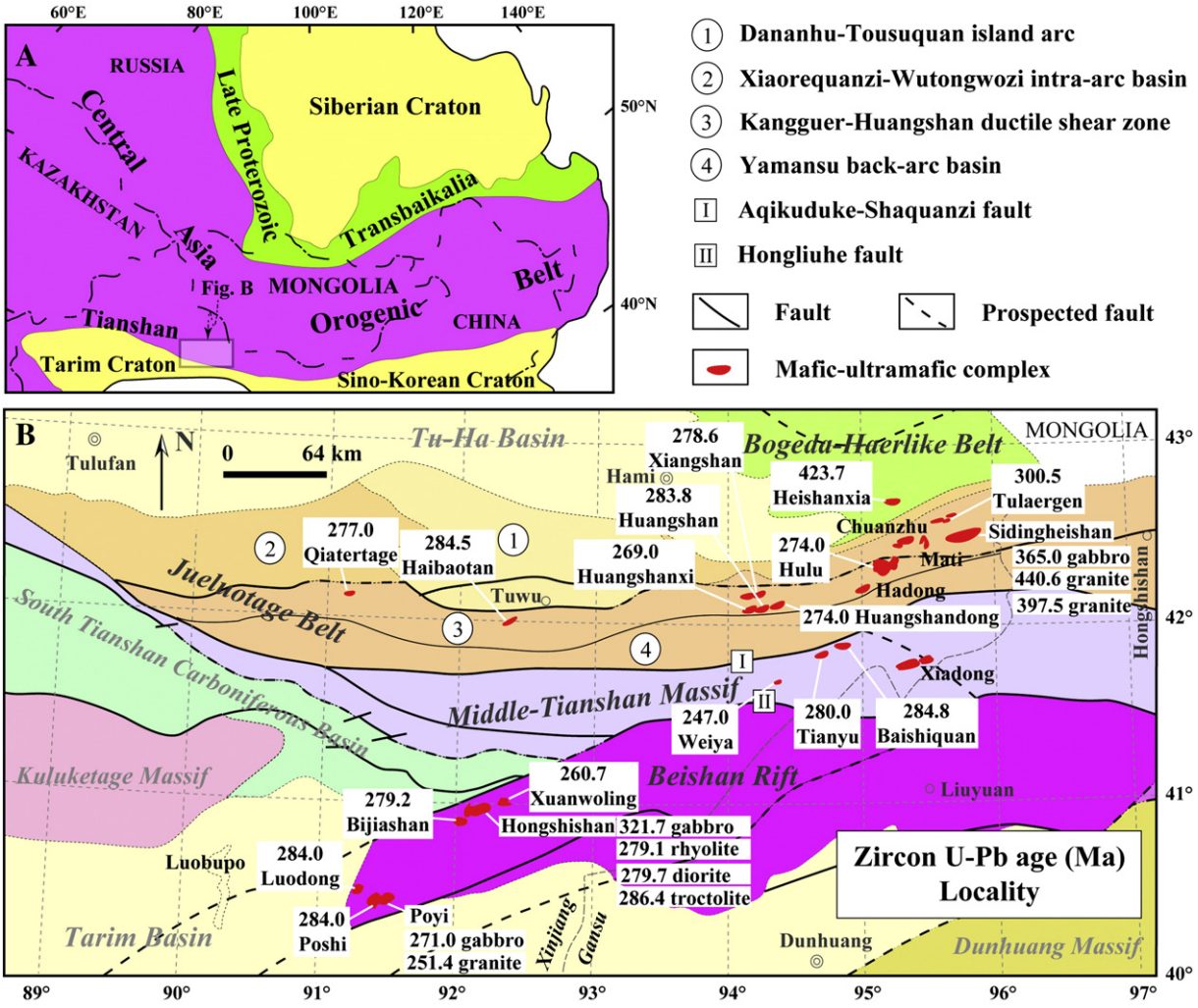

Fig. 1. (A) A geologic map of the study area, showing the location of the Eastern Tianshan and Beishan in the Central Asian Orogenic Belt (modified after Jahn et al., 2000b). (B) Regional geological map of the Eastern Tianshan and Beishan Rift showing the distribution and U–Pb ages of Paleozoic mafic–ultramafic complexes (modified after Su et al., 2011b). Age sources are from Qin et al. (2011) and Su et al. (2011b) and references therein.

The Eastern Tianshan and Beishan are key components of the CAOB, and are characterized by the exposure of numerous mafic–ultramafic complexes, most of which host Ni–Cu sulfide ore deposits (Fig. 1B; Qin et al., 2002, 2007; Zhou et al., 2004; Mao et al., 2008; Pirajno et al., 2008; Su et al., 2009, 2010, 2012a, b, c; Song et al., 2011). These complexes are 424 Ma to 247 Ma (Fig. 1B; Su et al., 2011b and reference therein) and are considered to have evolved from basaltic magmas (e.g., Li et al., 2006; Pirajno et al., 2008; Su et al., 2010, 2011c, 2012a; Tang et al., 2011; Zhou et al., 2004). Thus, they provide a perfect opportunity to probe into the nature and compositional evolution of the late Paleozoic mantle beneath these regions.

Bulk Nd–Sr and zircon Hf–O isotopes are powerful geochemical tracers for source and petrogenetic studies. They are widely used to recognize the nature and involvement of recycled crustal components in the mantle sources (e.g., Turner et al., 1997; Valley et al., 1998), to further identify whether the subducted materials are derived from oceanic or continental crust (Arndt et al., 1998; James, 1981; Magaritz et al., 1978; Wang et al., 2009a, 2009c; Zhang et al., 2009; Zhao and Zhou, 2007), and to discuss the geological processes such as crust–mantle interaction, petrogenesis and subduction (e.g., Rollinson, 1993; Wang et al., 2006; Zhang et al., 2009; Zhou et al., 2008). Furthermore, Nd–Sr and zircon Hf–O isotopic mapping have already been applied to the study of mantle heterogeneity and subduction-related magmatism (e.g., Su et al., 2011b; Turner et al., 1997; Wang et al., 2009a, 2009c; Zhou et al., 2008).

In this paper, we use 120 whole rock Rb–Sr, Sm–Nd isotopic analyses, and a summary of 347 published zircon Hf–O isotopes from 17 samples of mafic–ultramafic complexes in the Eastern Tianshan (including Jueluotage Belt and Middle Tianshan Massif) and Beishan to map the isotopic variations. The ages of the samples have already been determined by U–Pb zircon dating (Fig. 1; Appendix Table; Qin et al., 2011; Su et al., 2011b). This study improves our understanding of the mantle sources and origin of these complexes, particularly the compositional variations of the mantle beneath the southern CAOB.

2. Geological setting

The study area includes Eastern Tianshan and Beishan, which are located in the southern CAOB (Fig. 1A). The Eastern Tianshan, which forms the eastern part of Tianshan Mountains, mainly consists of three tectonic units: Bogeda–Haerlike Belt in the north, Jueluotage Belt in the center and Middle Tianshan Massif in the south (Fig. 1B; BGMRXUAR, 1993; Xu et al., 2009). The Jueluotage Belt can be subdivided, from north to south, into Wutongwozi–Xiaorequanzi intra-arc basin, Dananhu–Tousuquan island arc, Kangguer–Huangshan ductile shear zone and Yamansu back-arc basin (Fig. 1B; Qin et al., 2002).

The Bogeda–Haerlike Belt is made up of well developed Ordovician–Carboniferous volcanic rocks, granites and mafic–ultramafic complexes (BGMRXUAR, 1993; Gu et al., 2001; Li et al., 2006). The representative

mafic–ultramafic complex in the Bogeda–Haerlike Belt is called the Heishanxia complex (Fig. 1B; Su et al., 2011b), which consists of peridotite, olivine/plagioclase pyroxenite, gabbro and diorite.

The Jueluotage Belt is characterized by Middle Paleozoic volcanic and sedimentary strata, including subaerial volcanics, sandstones and pelitic slates with inter-layered limestones, mudstones, siltstones and conglomerates (BGMRXUAR, 1993). Carboniferous–Permian magmatism was active and resulted in the emplacement of copper- and gold-rich, high-potassium, relatively oxidized, calc-alkaline to alkali magmas (Qin et al., 2002, 2003; Xu et al., 2009). Abundant mafic–ultramafic complexes are largely distributed along deep fractures in the Kangguer–Huangshan ductile shear zone (Fig. 1B), and are significant magmatic Ni–Cu sulfide deposits (Han et al., 2010; Mao et al., 2008; San et al., 2010; Wang et al., 2009b; Xiao et al., 2010).

The Middle Tianshan Massif is composed of Precambrian crystalline basement (BGMRXUAR, 1993; Qin et al., 2002), and is bounded by the Aqikuduke–Shaquanzi Fault in the north and the Hongliuhe Fault in the south (Fig. 1B). Abundant granites and granitic gneisses outcrop as Precambrian crystalline basement of this massif (BGMRXUAR, 1993; Qin et al., 2002; Xu et al., 2009). Permian mafic–ultramafic complexes, including the Tianyu, Baishiquan and other mafic bodies are distributed along the northern margin of the Middle Tianshan Massif (Fig. 1B). The complexes here are very similar to those in the Jueluotage Belt in terms of petrology, mineralogy and mineralization, which usually display pervasive hydrothermal alteration in the Ni–Cu sulfide ore-bearing rocks (Chai et al., 2008; Liu et al., 2010; Mao et al., 2008; Song et al., 2011; Tang et al., 2009, 2011).

The Beishan Rift is located in the northeastern part of the Tarim Basin, adjacent to the Middle Tianshan Massif in the north (Fig. 1B; BGMRXUAR, 1993; Xu et al., 2009). It is mainly comprised of Precambrian crystalline basement and overlying sedimentary rocks, which encompass the Beishan, Gutongjing, Yangjibulake and Aierlanjigan groups. The Precambrian to Permian strata in the Beishan region are separated by well-developed fault-related uplifts and sags (Su et al., 2010, 2011a, c; Xu et al., 2009; Yue et al., 2001). Late Paleozoic tectonic evolution in this region is closely related to the subduction and subsequent closure of the South Tianshan Ocean, with the latter being described as a complicated process (e.g., Gao et al., 1998, 2006, 2009; Xiao et al., 2003, 2004a, 2009; Yue et al., 2001; Zhang et al., 2002). The rift was developed in the Carboniferous and Permian, accompanied by intermediate-basic volcanic eruptions (BGMRXUAR, 1993; Su et al., 2012a). The Permian mafic–ultramafic complexes discovered so far are predominately distributed in the western part of the rift, and intruded into the Proterozoic and Carboniferous strata (Jiang et al., 2006; Su et al., 2009, 2010, 2012a; Xu et al., 2009).

3. Characteristics of mafic–ultramafic complexes and their U–Pb ages

Mafic–ultramafic complexes in the Jueluotage Belt occur as east–west trending sills or dykes with areal extent of less than 3 km^2. The rock types include hornblende/pyroxene peridotite, olivine/amphibole pyroxenite, hornblende/olivine gabbro, norite and diorite (Han et al., 2010; Qin et al., 2002; Xiao et al., 2010). Generally, the ultramafic rocks occur in the center of the complexes and are surrounded by mafic bodies. All the rock types are variably altered and usually contain hydrous minerals, mostly hornblende with minor biotite (Liu et al., 2010; Zhou et al., 2004). Ni–Cu sulfide deposits being mined in the Jueluotage Belt are chiefly magma conduit type (Liu et al., 2010; Mao et al., 2008; San et al., 2010; Sun et al., 2007). The massive sulfide ore bodies are hosted by ultramafic rocks, while net-textured and disseminated sulfide ores are commonly observed in hornblende gabbro and norite (Han et al., 2010; Liu et al., 2010; San et al., 2010; Xiao et al., 2010). Most of the mafic–ultramafic complexes have zircon U–Pb ages between 300 Ma and 270 Ma (zircon U–Pb dating on SIMS) (Fig. 1B; Su et al., 2011b and reference therein) whereas a few formed earlier such as Heishanxia at 424 Ma (zircon U–Pb dating) and Sidingheishan at around 365 Ma (zircon U–Pb dating) (Su et al., 2011b).

The Baishiquan and Tianyu mafic–ultramafic complexes are located in the northern margin of the Middle Tianshan Massif and on the southern side of the Aqikuduke–Shaquanzi Fault (Fig. 1B). Both complexes are mainly composed of olivine pyroxenite, pyroxene peridotite, diorite, norite and gabbro, and host Ni–Cu sulfide deposits (Chai et al., 2008; Mao et al., 2006; Mao et al., 2008; Tang et al., 2009). Biotite is a common mineral phase in all the rocks. Zircons from gabbros yielded U–Pb ages of 285–280 Ma, respectively (Fig. 1B; Su et al., 2011b; Qin et al., 2011). The Weiya mafic body, consisting of gabbro, was formed in the Late Permian and hosts Ti–V–Fe oxide deposit (Wang et al., 2009b; Zhang et al., 2007). The Xiadong mafic–ultramafic complex has been identified as an Alaskan-type intrusion formed in the Carboniferous (Su et al., 2012b).

Mafic–ultramafic complexes in the Beishan Rift mostly extend E–W with their outcrops covering an area of less than 15 km^2, which is much larger compared with those in the Eastern Tianshan (Ao et al., 2010; Su et al., 2009, 2010, 2011b, c, 2012a, c). They have rock assemblage of dunite, pyroxene peridotite, troctolite, olivine gabbro and gabbro, most of which are fresh or slightly altered (Jiang et al., 2006; Su et al., 2009, 2010, 2011b). Plagioclase is commonly found in all rock types, but hydrous minerals are rarely present and merely observed in Poshi and Poyi complexes. Coeval volcanic rocks and felsic intrusions commonly coexist with the mafic–ultramafic complexes (Su et al., 2009, 2011a). Zircon U–Pb ages of the complexes and related volcanic rocks range from 286 Ma to 260 Ma (Fig. 1B; Su et al., 2011b; Qin et al., 2011). Ni–Cu mineralization in the Beishan complex is not as good as those in the Jueluotage Belt and Middle Tianshan Massif.

4. Analytical methods

About 100–200 mg of the whole rock powder was weighed into 7 ml Savillex™ Teflon beakers, and appropriate amounts of mixed ^{87}Rb–^{84}Sr and ^{149}Sm–^{150}Nd spikes were added. The samples were dissolved using a mixture of 2 ml HF and 0.2 ml $HClO_4$ on a hotplate at 120 °C for more than 1 week. After the samples were completely dissolved, the solutions were dried on a hotplate at 130–180 °C to evaporate the HF and $HClO_4$. The sample residues were re-dissolved in 4 ml of 6 M HCl, and dried again. Finally, the samples were dissolved in 5 ml of 3 M HCl.

After that, the solutions were loaded onto pre-conditioned Eichrom LN (LN-C-50A, 100–150 mm, 2 ml) chromatographic columns. The Rb, Sr, Sm, Nd, and matrix elements were eluted with 3 M HCl. The Sr and Nd collections from the LN columns were dried and re-dissolved in 1 ml 2.5 M HCl, and subsequently loaded onto pre-conditioned cation exchange columns packed with AG50W × 12 resins (200–400 mesh, 2 ml). Rb and Sr were stripped with 5 M HCl, and then REE were stripped with 6 M HCl. The REE collections were dried and re-dissolved in 0.4 ml 0.25 M HCl, after which the solutions were loaded onto pre-conditioned Eichrom LN (LN-C-50B, 100–150 mm, 2 ml) chromatographic columns. The La, Ce and a portion of the Pr were eluted with 6 ml 0.25 M HCl, the Nd was stripped with 3 ml 0.4 M HCl, and the Sm was stripped with 4 ml 0.8 M HCl. Procedural blanks were <200 pg for Sr and <50 pg for Nd.

For the measurements of isotopic compositions, Sr was loaded with a Ta–HF activator on a single W filament and Nd was loaded as phosphates and measured in a Re-double-filament configuration. $^{143}Nd/^{144}Nd$ ratios were normalized to $^{146}Nd/^{144}Nd = 0.7219$ and $^{87}Sr/^{86}Sr$ ratios to $^{86}Sr/^{88}Sr = 0.1194$. Isotopic ratios were measured on an IsoProbe-T thermal ionization mass spectrometer in the Laboratory for Radiogenic Isotope Geochemistry, Institute of Geology and Geophysics, Chinese Academy of Sciences. The procedure for chemical separation

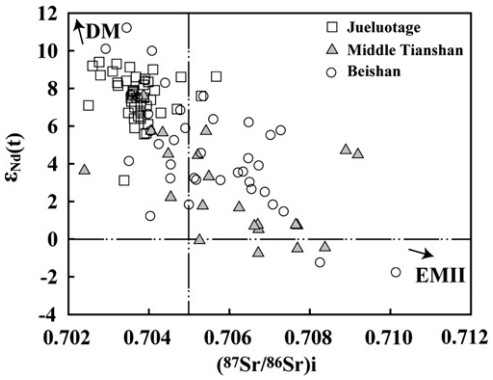

Fig. 2. ε_{Nd} (t) vs. $(^{87}Sr/^{86}Sr)i$ diagram for mafic–ultramafic complexes in the Jueluotage, Middle Tianshan and Beishan. DM, depleted mantle; EMII, enriched mantle II; ε_{Nd} (t) = 0 and $(^{87}Sr/^{86}Sr)_i = 0.705$ are values of bulk silicate Earth (Zindler and Hart, 1986).

and isotopic measurement followed that of Zhang et al. (2001) and Chu et al. (2009).

5. Analytical results and isotopic mapping

5.1. Bulk Nd–Sr isotopic results and mapping

New and previously published Nd and Sr isotopic data are presented in Appendix Table and illustrated in Fig. 2. On a broader scale, the $\varepsilon_{Nd}(t)$ values show large variations from −2 to +11, while the initial Sr isotopic ratios $(^{87}Sr/^{86}Sr)_i$ vary from 0.702 to 0.710 and correlate negatively with $\varepsilon_{Nd}(t)$ (Fig. 2). More specifically, the mafic–ultramafic rocks from the Jueluotage Belt have relatively restricted Nd–Sr isotopic variations: high $\varepsilon_{Nd}(t)$ between +5.5 and +9.5 (except for one sample) and low $(^{87}Sr/^{86}Sr)_i$ between 0.702 and 0.706 (Appendix Table; Figs. 2 and 3). On the $\varepsilon_{Nd}(t)$ vs. $(^{87}Sr/^{86}Sr)_i$ diagram (Fig. 2), the Middle Tianshan mafic–ultramafic intrusions are scattered,, whereas the mafic–ultramafic complexes and related rocks in the Beishan Rift have the largest Nd–Sr isotopic variations: $\varepsilon_{Nd}(t)$ of −2–+11 and $(^{87}Sr/^{86}Sr)_i$ of 0.703–0.710 (Figs. 2 and 3).

Spatially, the $(^{87}Sr/^{86}Sr)_i$ ratios of mafic–ultramafic complexes increase southward from the Jueluotage Belt to the Middle Tianshan Massif, while the $\varepsilon_{Nd}(t)$ values show an opposite trend (Figs. 3 and 4). Within the Beishan Rift, the complexes exhibit clear

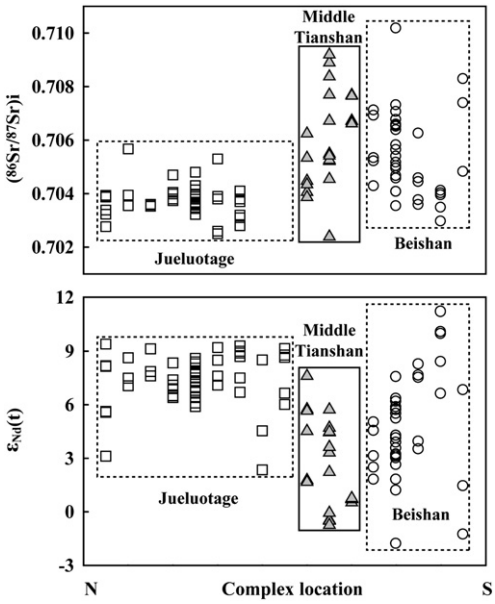

Fig. 4. Spatial variations in $(^{87}Sr/^{86}Sr)_i$ and ε_{Nd} (t) of the mafic–ultramafic complexes. Complexes were projected onto the section based on their location in the Jueluotage, Middle Tianshan and Beishan.

northeastward increase in $(^{87}Sr/^{86}Sr)_i$ ratios and decrease in $\varepsilon_{Nd}(t)$ values from Luodong to Xuanwoling, a trend that could possibly extend to the complexes in the Middle Tianshan Massif (Figs. 3 and 4).

5.2. Zircon Hf–O isotopic mapping

Zircon Hf–O data in Table 1 are summarized from Su et al. (2011a, b). Zircons separated from the mafic–ultramafic intrusions display oscillatory, patchy and concentric or linear zoning, and have Th/U ratios of >0.10, indicating they are not xenocrysts but actually crystallized from the mafic or ultramafic magmas. The mafic–ultramafic complexes in the Jueluotage Belt show wide variations in zircon Hf and O isotopic compositions: $^{176}Hf/^{177}Hf = 0.282737–0.283066$, corresponding to ε_{Hf} (t) = +6.0–+17.0, and $\delta^{18}O = 4.14‰–8.00‰$ (Table 1; Figs. 5 and 6; Su et al., 2011b). Most of the zircons have Hf model ages ranging from 600 Ma to 300 Ma (Figs. 5 and 7), and $\delta^{18}O$ values lower than

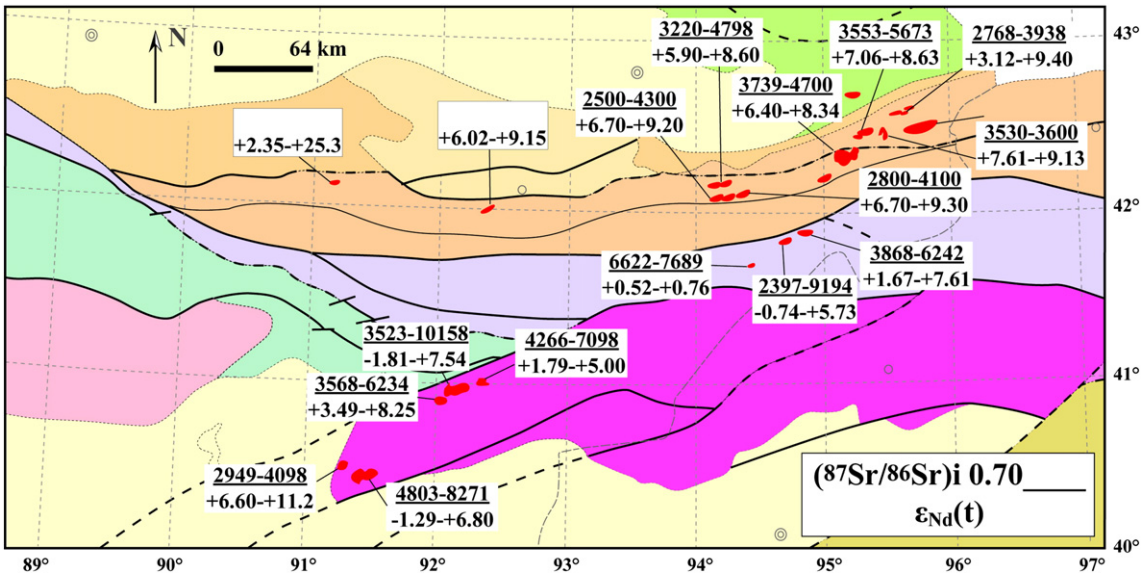

Fig. 3. Nd–Sr isotopic map for mafic–ultramafic complexes in the Jueluotage, Middle Tianshan and Beishan.

Table 1
Zircon Hf–O isotopic compositions of the mafic–ultramafic complexes from the Jueluotage Belt, Middle Tianshan Massif and Beishan Rift.

Sample	Rock type	Complex	$^{176}Lu/^{177}Hf$	$^{176}Hf/^{177}Hf$	$^{176}Hf/^{177}Hf_i$	ε_{Hf} (t)	T_{DM} (Ma)	$\delta^{18}O$
Jueluotage Belt								
HSX	Gabbro	Heishanxia	0.000156–0.001218	0.282820–0.282902	0.282819–0.282896	11.0–13.7	493–600	5.17–5.90
TLG-V2	Gabbro	Tulaergen	0.000872–0.002519	0.282737–0.282939	0.282727–0.282923	6.27–13.2	462–740	4.71–6.08
SH-11	Granite	Sidingheishan	0.001626–0.005040	0.282881–0.283019	0.282866–0.282997	12.1–16.7	350–542	4.14–5.29
SH-R	Granite	Sidingheishan	0.001529–0.004449	0.282864–0.283006	0.282843–0.282977	12.2–17.0	374–574	
SH-V	Gabbro	Sidingheishan	0.000393–0.000764	0.282869–0.282937	0.282865–0.282933	11.3–13.7	442–538	
XSCuNi-V	Gabbro	Xiangshan	0.000796–0.002561	0.282907–0.283066	0.282902–0.283056	10.8–16.3	305–490	4.35–5.49
XSTiFe-V	Gabbro	Xiangshan	0.000697–0.003855	0.282860–0.283047	0.282853–0.283035	8.98–15.4	300–562	6.09–7.43
HS-V	Gabbro	Huangshan	0.000721–0.004532	0.282763–0.282996	0.282738–0.282987	5.05–13.8	370–766	5.19–8.00
Middle Tianshan Massif								
BSQ-V	Gabbro	Baishiquan	0.000311–0.001862	0.282640–0.282813	0.282636–0.282808	1.36–7.47	621–862	
TY-V	Gabbro	Tianyu	0.000484–0.002665	0.282688–0.282820	0.282677–0.282814	2.81–7.64	616–822	5.17–6.30
Beishan Rift								
XWL-V	Gabbro	Xuanwoling	0.000342–0.001653	0.282622–0.282809	0.282616–0.282805	0.21–6.89	625–899	5.75–6.75
HS139	Troctolite	Hongshishan	0.000275–0.002695	0.282850–0.283008	0.282847–0.283006	8.93–14.6	339–565	4.96–8.31
HSS6	Rhyolite	Hongshishan	0.000558–0.006239	0.282609–0.283075	0.282606–0.283068	0.26–16.6	427–901	4.33–10.3
HSS12	Diorite	Hongshishan	0.001341–0.005139	0.282634–0.282831	0.282621–0.282818	0.79–7.77	622–912	6.57–10.3
BJS6	Gabbro	Bijiashan	0.001225–0.003851	0.282621–0.282849	0.282608–0.282835	0.32–8.35	600–934	5.02–11.9
PSZK1-2-650	Gabbro	Poshi	0.001666–0.003555	0.282650–0.283015	0.282641–0.283006	1.60–14.5	343–871	6.29–8.56
PY	Granite	Poyi	0.000343–0.001434	0.282600–0.282754	0.282594–0.282749	−0.78–4.71	706–932	6.16–7.01

Note: All data are summarized from Su et al. (2011a, b).

typical mantle zircon values of 5.3‰ ± 0.3‰ (Valley et al., 1998). Zircons from the Tianyu and Baishiquan gabbros in the Middle Tianshan Massif have $^{176}Hf/^{177}Hf$ ratios of 0.282640–0.282820, corresponding to ε_{Hf} (t) of +1.4–+7.6 with Hf model ages of 862–616 Ma (Fig. 6 and 7), and $\delta^{18}O$ values of 5.17‰–6.30‰ (Table 1; Fig. 5). The mafic–ultramafic complexes and related rocks in the Beishan Rift also show wide variations in zircon Hf and O isotopic compositions (Figs. 5 and 6) with $^{176}Hf/^{177}Hf$ ratios falling within the range of 0.282600–0.283075. Correspondingly, their ε_{Hf} (t) values vary between −1 and +17 with a concentrated distribution of 0–+9 (Table 1; Figs. 5 and 6). Hf model ages are mostly in the range of 900–600 Ma (Table 1), while the $\delta^{18}O$ values range from +4‰ to +12‰ with a peak between +6‰ and +8‰ (Figs. 5 and 7).

The spatial distribution shows that zircon ε_{Hf} (t) values display an apparent southward decreasing trend from the Jueluotage Belt, through Middle Tianshan, to Beishan Rift (Fig. 7). The Hf model ages show a continuous decrease from north to south within the Jueluotage Belt, and a similar trend is also observed from the southwestern-most complex in the Beishan Rift to the northeastern complex in the Middle Tianshan Massif (Figs. 6 and 7). Oxygen isotopes display overall southward increase in $\delta^{18}O$ values and large variations in the Beishan Rift (Figs. 5, 6 and 7).

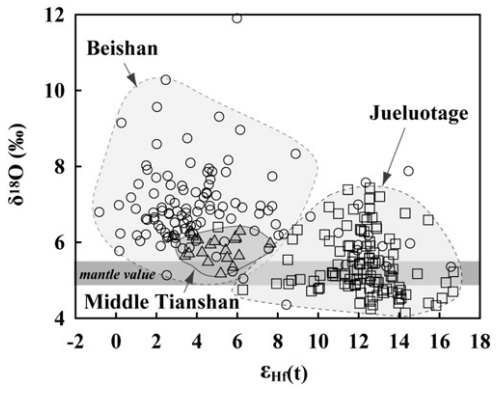

Fig. 5. ε_{Hf} (t) vs. $\delta^{18}O$ diagram for mafic–ultramafic complexes in the Jueluotage, Middle Tianshan and Beishan.
Mantle zircon O isotopic composition of $\delta^{18}O = 5.3‰ \pm 0.3‰$ is from Valley et al. (1998).

6. Discussion

6.1. Crustal contamination

Many studies have revealed S isotopic ($\delta^{34}S$) variations in major reservoirs of the earth such as: arc volcanic rocks, −0.2–+20.7‰; granite, −10–+15‰; mantle, 0 ± 3‰; continental crust, +7‰ (Chaussidon and Lorand, 1990; Coleman, 1977). In this aspect, sulfur isotopic system has been considered as an indicator of crustal assimilation. The Jueluotage mafic–ultramafic intrusions have $\delta^{34}S$ values of mostly +0.5–+5‰, overlapping the $\delta^{34}S$ range of +1.5–+6.5‰ of their country rocks (Sun, 2009). The Middle Tianshan intrusions have high $\delta^{34}S$ values ranging from +4‰ to +8.5‰, similar to or slightly higher than the $\delta^{34}S$ ranges (+3–+6.5‰) of the country rocks (Tang, 2009). Both mafic–ultramafic rocks and country rocks in the Beishan area show restricted sulfur isotopic values ($\delta^{34}S$ = −2‰–+2‰) within mantle range (Su, 2010). We thus suggest that crustal assimilation did not significantly modify the geochemical compositions of parental magmas of the Eastern Tianshan and Beishan intrusions.

Studies have shown that mantle-derived magmas could be contaminated by crustal materials either along their ascending conduit or within their sources. Some trace element ratios are useful proxies to evaluate the extent of crustal contamination. For example, the presence of negative Nb and Ta anomalies could be related to crustal assimilation or subduction component in a mantle source (Arndt et al., 1998; Zhou et al., 2009). Ratios of primitive mantle-normalized trace element contents such as $(Ta/Th)_{PM}$ and $(Nb/Th)_{PM}$ are indicators of the extent of Ta and Nb anomalies, whereas $(Th/Yb)_{PM}$ is a sensitive indicator of crustal contamination (e.g., Wang and Zhou, 2006; Zhang et al., 2009). Compared to N-MORB (normal mid-oceanic ridge basalt), the mafic–ultramafic rocks from the Jueluotage, Middle Tianshan and Beishan complexes have very low $(Ta/Th)_{PM}$ and $(Nb/Th)_{PM}$ but high $(Th/Yb)_{PM}$ ratios, indicating variable degrees of crustal contamination (Fig. 8A, B). However, the crustal contamination trend seems to have no chemical affinity with either lower or upper continental crustal components as demonstrated in diagrams of $(Th/Yb)_{PM}$ vs. $(Nb/Th)_{PM}$ and Nb/La vs. Nb/Th (Fig. 8B, C). Furthermore, the high La/Nb and low La/Ba ratios of the mafic–ultramafic rocks imply that they were possibly derived from subduction-modified mantle sources (Fig. 8D).

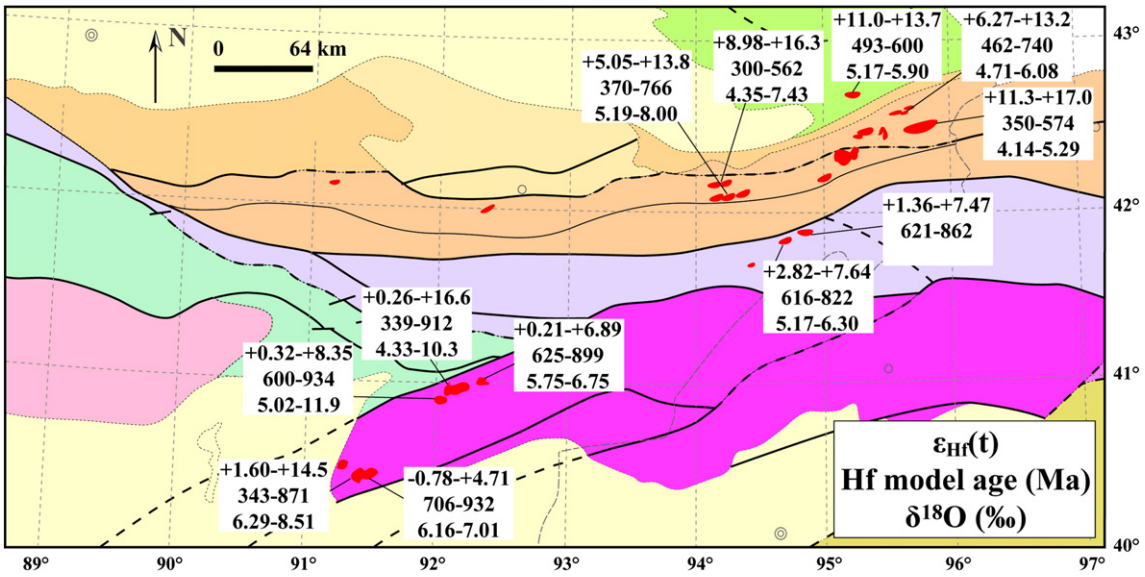

Fig. 6. Zircon Hf–O isotopic and Hf model age map for mafic–ultramafic complexes in the Jueluotage, Middle Tianshan and Beishan.

The Sr–O isotope correlation diagram has been broadly adopted to distinguish crustal contamination mechanisms, such as contamination in mantle source or crustal assimilation during magma ascent, since crustal materials have much higher Sr abundance and $^{87}Sr/^{86}Sr$ ratio relative to the mantle, while O concentrations are similar in almost all rock types (e.g., Magaritz et al., 1978; James, 1981; Rollinson, 1993 and reference therein). The bulk $(^{87}Sr/^{86}Sr)_i$ and zircon $\delta^{18}O$ values of the mafic–ultramafic rocks from the Jueluotage, Middle Tianshan and Beishan complexes are distributed below or close to the convex-downward mixing line (Fig. 9), which represents a source contaminated by crust/slab fluid. Trace elemental and Sr–O isotopic features indicate that significant crustal contamination occurred in the mantle sources rather than along ascending conduit of the mafic–ultramafic magmas which gave rise to the formation of the Eastern Tianshan and Beishan complexes. Consequently, the Nd–Sr–Hf–O isotopes of the mafic–ultramafic complexes can be used to trace their mantle sources and magmatic processes.

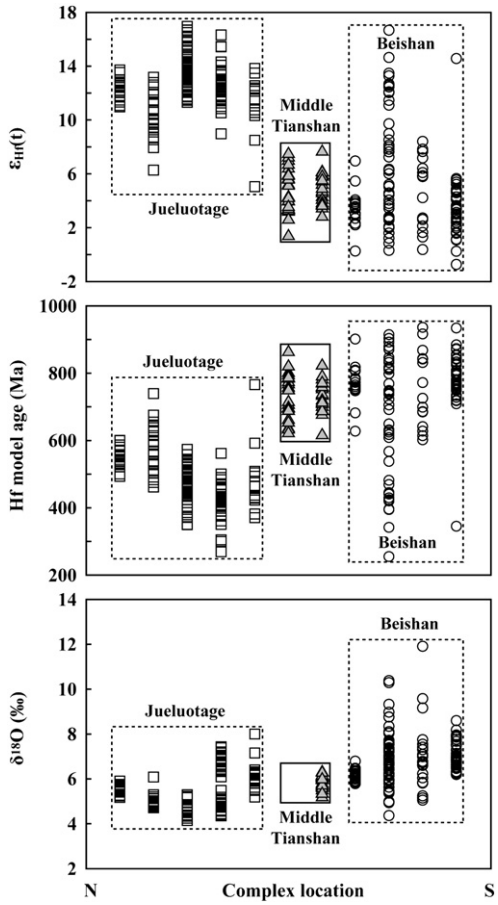

Fig. 7. Spatial variations in zircon $\varepsilon_{Hf}(t)$, Hf model age and $\delta^{18}O$ of the mafic–ultramafic complexes. Complexes were projected onto the section based on their location in the Jueluotage, Middle Tianshan and Beishan.

6.2. Compositional heterogeneity of the mantle sources

As shown the mafic–ultramafic complexes in the Jueluotage Belt have restricted Nd–Sr–Hf–O isotopic variations (Figs. 2–7), implying that their mantle sources are almost isotopically homogenous. Their high $\varepsilon_{Nd}(t)$ and $\varepsilon_{Hf}(t)$, low $(^{87}Sr/^{86}Sr)_i$ (Figs. 2 and 5) and mantle-level $\delta^{18}O$ values (Fig. 5) indicate that the mantle sources possess depleted isotopic signatures close to the depleted mantle (DM) reservoir (Fig. 2; Zindler and Hart, 1986). The mafic–ultramafic rocks in the Middle Tianshan Massif display large variations in Nd–Sr isotopes (Figs. 2 and 4) but narrow Hf–O isotopic ranges (Fig. 7). In contrast, extremely large variations in all relevant isotopes of the mafic–ultramafic complexes in the Beishan Rift (Figs. 2, 4, 5, and 7) reflect conspicuous compositional heterogeneity of their mantle sources ranging from DM to enriched mantle II (EM-II) (Fig. 2; Zindler and Hart, 1986; Su et al., 2011b, 2012a).

Taking the whole dataset into consideration, the mantle sources of the mafic–ultramafic complexes in the Eastern Tianshan and Beishan have spatially heterogeneous Nd–Sr–Hf–O isotopic compositions (Figs. 3 and 6), which is evident by the negative correlations of $(^{87}Sr/^{86}Sr)_i$ vs. $\varepsilon_{Nd}(t)$ (Fig. 2) and $\varepsilon_{Hf}(t)$ vs. $\delta^{18}O$ (Fig. 4), suggesting a mixing trend from DM to EM-II. In addition, several previous studies have attributed the mantle heterogeneity, especially the formation of EM-II reservoir, to subduction-related modification (e.g., Rollinson, 1993; Su et al., 2012a; Turner et al., 1997; Zhou et al., 2004; Zindler and Hart, 1986). Accordingly, we can conclude with high level of certainty that the mantle beneath the Eastern Tianshan and Beishan had been strongly modified to variable extents by subduction-related processes during the Paleozoic.

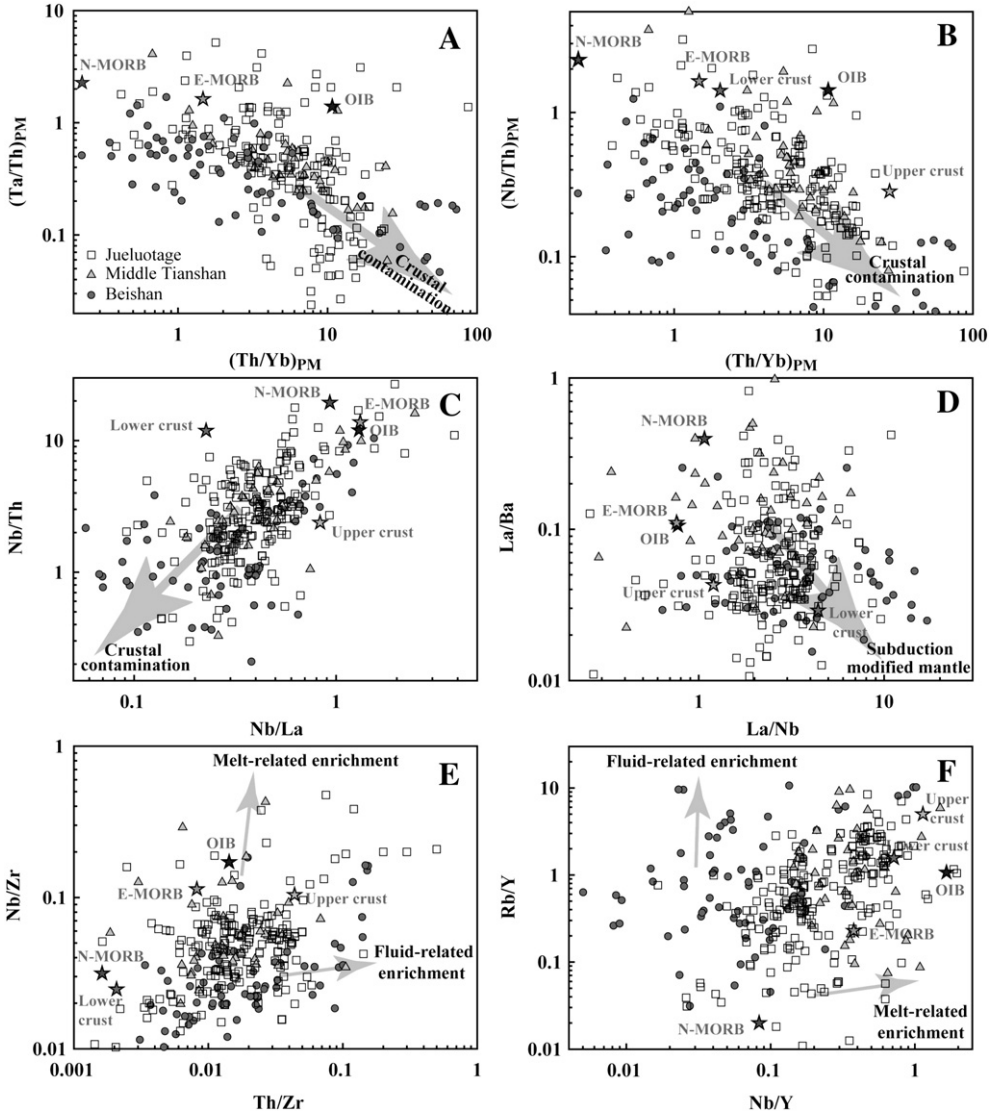

Fig. 8. Correlated diagrams of trace element ratios of the mafic–ultramafic complexes in the Eastern Tianshan and Beishan. $(Ta/Th)_{PM}$, $(Th/Yb)_{PM}$, $(Nb/Th)_{PM}$ are primitive mantle (PM) normalized values.
Data sources for PM, OIB, N-MORB, E-MORB, Upper crust, Lower crust values are from Sun and McDonough (1989). Trace element data of mafic–ultramafic complex are from Zhou et al. (2004), Jiang et al. (2006), Li et al. (2006), Chai et al. (2008), Xia et al. (2008), Sun (2009), Tang (2009), Tang et al. (2009, 2011), Xiao et al. (2010), Su et al. (2010, 2011b, 2012a).

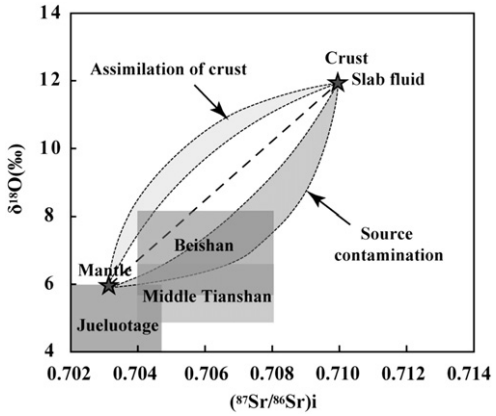

Fig. 9. $^{87}Sr/^{86}Sr$ vs. $\delta^{18}O$ diagram illustrating the effects of source and crustal contamination on Sr and O isotope concentrations in a mantle melt. The mantle source has $^{87}Sr/^{86}Sr = 0.703$ and $\delta^{18}O = 6.0‰$; the contaminant (crust/slab fluid) has $^{87}Sr/^{86}Sr = 0.710$ and $\delta^{18}O = 12‰$ (James, 1981).

6.3. Subduction modification in the mantle source

The geology of the Jueluotage Belt is characterized by distinct volcanic rock types and related mineralization in each tectonic unit. For example, the Dananhu–Tousuquan island arc is characterized by Devonian and Early Carboniferous andesites and porphyry copper deposit-hosting granite intrusions (e.g., Tuwu-Yandong; Zhang et al., 2004); the Kangguer–Huangshan ductile shear zone consists of metamorphosed Carboniferous volcanic rocks and tuff, and hosts orogenic lode-type gold deposits (Qin et al., 2002, 2003); the Yamansu belt has distributions of calc-alkaline volcanics, granitoids and many Fe- and Cu-bearing deposits in volcanic rocks and has been distinguished as a back arc basin in Carboniferous (Qin et al., 2002). Additionally, the discovery of an Alaskan-type Xiadong mafic–ultramafic complex in the Middle Tianshan Massif suggests the presence of a continental arc during the early Paleozoic (Su et al., 2012b, c). The Hf model ages of zircons from the mafic–ultramafic complexes in the Jueluotage Belt mainly fall within the range of 600 Ma–310 Ma (Fig. 7; Su et al., 2011b). The above features can be explained by the southward subduction of the Junggar Ocean beneath the study area

during the Paleozoic and subsequently closed at around Late Carboniferous. Because the subducted materials were mainly Paleozoic volcanic rocks that have depleted Nd–Sr–Hf–O isotopic compositions, they would not greatly change the isotopic systems of the overlying mantle wedge, thus the mafic–ultramafic complexes in the Jueluotage belt show relatively restricted Nd–Sr–Hf–O isotopic compositions, similar to the depleted mantle.

The oldest blueschist along the South Tianshan and the youngest ophiolite in the Beishan Rift reported so far are around 900 Ma and 420 Ma old respectively (Mao, 2008; Nakajima et al., 1990), which are consistent with the zircon Hf model age of the mafic–ultramafic complexes (900 Ma–400 Ma) in the Beishan Rift. The increasing $(^{87}Sr/^{86}Sr)_i$ and decreasing ε_{Nd} (t) from south to north (Fig. 4) imply the northward subduction of the South Tianshan Ocean during the period of 900 Ma–400 Ma (Su et al., 2011b). The relatively ancient and long-lived subduction event and the occurrence of Precambrian basement in the Beishan region may explain the highly variable Nd–Sr–Hf–O isotopic compositions.

Although the mantle sources beneath Eastern Tianshan and Beishan had both been modified by subducted materials, Ni–Cu mineralization of the mafic–ultramafic complexes from these two locations are completely different, with abundant deposits hosted in the Jueluotage Belt but are rarely found in the Beishan. This disparity may be directly correlated with distinct types of modification which could be discriminated by trace element ratios. Compared with LILE such as Th and Rb, HFSE (e.g., Zr, Nb) are relatively immobile in aqueous fluids (e.g., Turner et al., 1997). Firstly, Nb/Zr and Nb/Y ratios will change as functions of source compositions, but the addition of fluid components from subducted slab to the mantle wedge will not significantly affect them (e.g., Pearce and Peate, 1995). Secondly, mantle sources modified by slab melts are likely to have lower Th/Zr and Rb/Y ratios than those modified by fluids (e.g., Zhao and Zhou, 2007). The higher Th/Zr and Rb/Y ratios at given Nb/Zr and Nb/Y ratios in the Beishan mafic–ultramafic rocks (Figs. 8E, F) indicate that the magmas were probably derived from mantle sources strongly modified by hydrous fluids. On the other hand, the positive correlations of Th/Zr vs. Nb/Zr and Nb/Y vs. Rb/Y in the Jueluotage and Middle Tianshan mafic–ultramafic rocks (Fig. 8E, F) suggest that their mantle sources had been modified by both slab fluids and melts.

The mafic–ultramafic complexes in the Middle Tianshan Massif have similar bulk Nd–Sr and zircon Hf isotopic variations to those in the Beishan Rift (Figs. 2–7). In addition, the Middle Tianshan mafic–ultramafic rocks have identical rock assemblage, Ni–Cu mineralization, trace element and zircon O isotopic compositions to those in the Jueluotage Belt (Figs. 5, 8, and 9; Su et al., 2012b). Particularly, the bulk Nd–Sr and zircon Hf–O isotopes display systematic variations for the Jueluotage, Beishan and Middle Tianshan (Figs. 3, 4, 6, and 7). As discussed above, the Nd–Sr–Hf–O signatures overprinted in the Beishan mafic–ultramafic intrusions are related to the subduction of the South Tianshan Ocean, whereas these signatures in the Eastern Tianshan intrusions are related to the Junggar oceanic subduction. The unique similarities of the Middle Tianshan mafic–ultramafic complexes could be well explained by subduction-related modifications to their mantle sources first by the early South Tianshan Ocean, followed by the Junggar Ocean.

6.4. Mechanism of generation of mafic–ultramafic magmas

6.4.1. Post-orogenic extension

Extensive studies on Carboniferous basalts, andesites, adakites and granitoids in north Xinjiang have revealed that these rocks display a conspicuous subduction component evidenced by positive bulk ε_{Nd} (t) and zircon ε_{Hf} (t) values (e.g., Sun et al., 2008; Tang et al., 2010, 2012; Xiao et al., 2011) and Geng et al. (2009, 2011) proposed a model of Junggar oceanic ridge subduction commenced from the Early Carboniferous. There is also a broad consensus that the Junggar ocean was closed in the Late Carboniferous and the Eastern Tianshan was in post-collisional extension setting since Early Permian evidenced by the discovery of the youngest ophiolite of ~310 Ma and widespread bimodal volcanic-sedimentary rocks (e.g., Gu et al., 2001; Li et al., 2010; Qin et al., 2002, 2003; Su et al., 2011b; Wang et al., 2006; Xu et al., 2009), although a few authors believe that the subduction might have lasted until Late Permian and Early Triassic based on their considering Permian mafic–ultramafic complexes as Alaskan-type complex formed in island arc setting (Ao et al., 2010; Xiao et al., 2004a). However, the discovery of alkaline granites and bimodal igneous series in the Beishan region suggests that the Beishan region once was a continental rift that developed in the early Permian (Su et al., 2011a). Zircons from the mafic–ultramafic complexes are mainly Early Permian in age, ranging from 290 Ma to 270 Ma (Fig. 1B). The distribution of these complexes is linear along west–east faults. For example, the Huangshan, Huangshandong and Xiangshan complexes are along the Kanggur suture; the Baishiquan and Tianyu deposits are along the Aqikuduke fault, whereas the Poyi, Poshi and Luodong intrusions are along the Baidiwa fault (Fig. 1B; Mao et al., 2008; Pirajno et al., 2008). Widespread magmatic metallogenesis in these regions occurred during post-collisional stages of the Late Carboniferous to Early Permian, and the Ni–Cu sulfide deposits in the mafic–ultramafic intrusions are just a product of this metallogenic event (Mao et al., 2008; Qin et al., 2002; Wang et al., 2006; Xu et al., 2009). Accordingly, the generation of mafic–ultramafic magmas can be temporally and spatially attributed to post-orogenic extension.

6.4.2. Early Permian mantle plume

Although post-orogenic extension contributes significantly to the generation of the mafic–ultramafic magmas, it is insufficient to explain some geological and geochemical features, such as: (1) the southwestward extension of most mafic–ultramafic bodies at depth, particularly in the Eastern Tianshan (e.g., San et al., 2010; Xiao et al., 2010), implying that the driving force for the ascent of their parental magmas were from the same direction, which cannot be explained by post-collisional extension but might be generated from a peripheral zone of the mantle plume; (2) the extremely high temperatures estimated to be in the range of 1100–1600 °C (Herzberg and O'Hara, 2002; Isley and Abbott, 2002; Su et al., 2009; Tang et al., 2006; Zhou et al., 2004) required for the low-Ti (1.8 wt.%) and high-Mg (>12 wt.%) parental magmas (Qin et al., 2011) since the generation of magmas in an extensional setting is generally decompression melting; (3) the identical formation ages of around 280 Ma for both the Eastern Tianshan and Beishan despite the quite different petrological, mineralogical and geochemical features between the mafic–ultramafic complexes in the two settings (Qin et al., 2011; Su et al., 2011b). (4) The commonly observed geochronological and geochemical correlations between the mafic–ultramafic complexes of the Eastern Tianshan and Beishan and basalts in the Tarim Basin (Qin et al., 2011).

Taking all this information into account, Zhou et al. (2004, 2009) proposed that the high temperature needed for the generation of high-Mg magmas could be provided by a mantle plume. However, Mao et al. (2006, 2008) suggested that the mafic–ultramafic intrusions might be the root of the erupted basalts which were eroded away afterwards in the Eastern Tianshan and Beishan Rift, but was preserved in the Tarim Basin. It has previously been established that the Beishan region was a Late Paleozoic rift probably developed in association with the early Permian mantle plume activity in the Tarim Basin (Qin et al., 2011; Su et al., 2011a, b). The Tarim basalts characterized by with high TiO_2, low MgO contents and negative ε_{Nd} (t) values have been interpreted to be derived from low-degree melting of asthenosphere and subsequently contaminated by Mesoproterozoic sedimentary rocks during their ascent (e.g., Zhang et al., 2008; Zhou et al., 2009), and thus were generated directly from a peripheral zone of the mantle plume, which is similar to the observations in the Emeishan and Southern African plumes (e.g., Jourdan et al., 2009;

Xiao et al., 2004b). The parental magmas of mafic–ultramafic intrusions were derived from the lithospheric mantle by high degree of melting due to the higher temperature of the mantle plume head (Qin et al., 2011; Su et al., 2011b, 2012a). Furthermore, rifts are commonly considered as surface responses to the uplift of the lithosphere overlying the mantle plume (e.g., Rogers et al., 2000; Saunders et al., 2005; Xu et al., 2001; Zhao et al., 2006). Therefore, the early Permian mantle plume might be situated closer to the Beishan Rift than the Eastern Tianshan and the western Tarim (Qin et al., 2011; Su et al., 2011b), which can explain why the mafic–ultramafic complexes from the Beishan Rift rather than other locations were evolved from anhydrous magma system evidenced by the occurrence of a great proportion of troctolites.

In summary, we suggest that it was the post-orogenic extension and ~280 Ma mantle plume event that generated the mafic–ultramafic magmas. The former provides space and conduit for magmas and plays a pivotal role in the Eastern Tianshan, while the latter supplies heat and contributes more to the Beishan Rift.

7. Conclusions

1) The mafic–ultramafic complexes in the Eastern Tianshan and Beishan Rift display identical petrological, mineralogical and mineralization signatures. On the other hand, the mafic–ultramafic complexes in the Jueluotage and Middle Tianshan have a relatively large proportion of hydrous minerals and commonly host Ni–Cu deposits. In contrast, the Beishan complexes are characterized by the occurrence of plagioclase-rich rocks and troctolites and are barren of Ni–Cu sulfide deposits.
2) The isotopic maps of the mafic–ultramafic complexes illustrates that there are increasing and decreasing trends for the $(^{87}Sr/^{86}Sr)_i$ and $\varepsilon_{Nd}(t)$ values, respectively, from the Jueluotage and Beishan to the Middle Tianshan. At the same time, the zircon Hf–O isotopes exhibit an apparent southward decrease in $\varepsilon_{Hf}(t)$ values and an increase in $\delta^{18}O$ values from north to south. These features suggest that the mantle sources of the late Paleozoic mafic–ultramafic complexes are evidently heterogeneous.
3) The Nd–Sr–Hf–O isotopic heterogeneity in the mantle beneath the Eastern Tianshan and Beishan probably resulted from subduction-related modification. The late Paleozoic mantle beneath the Jueluotage Belt was modified by both slab fluids and melts released during the subduction of the Junggar Ocean, whereas the mantle beneath the Beishan Rift was only subjected to fluid-related modification during the subduction of the South Tianshan Ocean. The mantle beneath the Middle Tianshan was modified by the early subduction of South Tianshan Ocean and subsequently the Junggar Ocean.
4) The mechanism for the generation of mafic–ultramafic magmas can be attributed to post-orogenic extension and ~280 Ma mantle plume event, with the former playing a more significant role in the Eastern Tianshan while the latter contributes more to the Beishan Rift.

Supplementary materials related to this article can be found online at doi:10.1016/j.lithos.2011.12.011

Acknowledgments

We are grateful for the constructive comments of two referees and sincerely thank professor A.C. Kerr for editorial handling. Funding by National Natural Science Foundation of China (Grants 41030424 and 41173011), Knowledge Innovation Program of the Chinese Academy of Sciences (Grant KZCX2-YW-Q04-08) and the China Postdoctoral Science Foundation (to Ben-Xun Su) is gratefully acknowledged.

References

Ao, S.J., Xiao, W.J., Han, C.M., Mao, Q.G., Zhang, J.E., 2010. Geochronology and geochemistry of Early Permian mafic–ultramafic complexes in the Beishan area, Xinjiang, NW China: implications for late Paleozoic tectonic evolution of the southern Altaids. Gondwana Research 18, 466–478.

Arndt, N.T., Chauvel, C., Fedorenko, V., Czamanske, G., 1998. Two mantle sources, two plumbing systems: tholeiitic and alkaline magmatism of the Maymecha River basin, Siberian flood volcanic province. Contributions to Mineralogy and Petrology 133, 297–313.

BGMRXUAR, 1993. Regional Geology of Xinjiang Uygur Autonomous Region. Geological Publishing House, pp. 1–841 (in Chinese).

Chai, F.M., Zhang, Z.C., Mao, J.W., Dong, L.H., Zhang, Z.H., Wu, H., 2008. Geology, petrology and geochemistry of the Baishiquan Ni–Cu-bearing mafic–ultramafic intrusions in Xinjiang, NW China: implications for tectonics and genesis of ores. Journal of Asian Earth Sciences 32, 218–235.

Chaussidon, M., Lorand, J.P., 1990. Sulphur isotope composition of orogenic spinel lherzolite massifs from Ariege (N.E. Pyrenees, France): an ion microprobe study. Geochimica et Cosmochimica Acta 54, 2835–2846.

Chu, Z.Y., Wu, F.Y., Walker, R.J., Rudnick, R.L., Pitcher, L., Puchtel, I.S., Yang, Y.H., Wilde, S.A., 2009. Temporal evolution of the lithospheric mantle beneath the eastern North China Craton. Journal of Petrology 50, 1857–1898.

Coleman, M.L., 1977. Sulphur isotopes in petrology. Journal of the Geological Society of London 133, 593–608.

Gao, J., Li, M.S., Xiao, X.C., Tang, Y.Q., He, G.Q., 1998. Paleozoic tectonic evolution of the Tianshan orogen, northwestern China. Tectonophysics 287, 213–231.

Gao, J., Long, L.L., Qian, Q., Huang, D.Z., Su, W., Klemd, R., 2006. South Tianshan: a late Paleozoic or a Triassic orogen. Acta Petrologica Sinica 22, 1049–1061 (in Chinese with English abstract).

Gao, J., Long, L.L., Klemd, R., Qian, Q., Liu, D.Y., Xiong, X.M., Su, W., Liu, W., Wang, Y.T., Yang, F.Q., 2009. Tectonic evolution of the South Tianshan orogen and adjacent regions, NW China: geochemical and age constraints of granitoid rocks. International Journal of Earth Sciences 98, 1221–1238.

Geng, H.Y., Sun, M., Yuan, C., Xiao, W.J., Xian, W.S., Zhao, G.C., Zhang, L.F., Wong, K., Wu, F.Y., 2009. Geochemical, Sr–Nd and zircon U–Pb–Hf isotopic studies of Late Carboniferous magmatism in the West Junggar, Xinjiang: implications for ridge subduction? Chemical Geology 266, 373–398.

Geng, H.Y., Sun, M., Yuan, C., Zhao, G.C., Xiao, W.J., 2011. Geochemical and geochronological study of early Carboniferous volcanic rocks from the West Junggar: petrogenesis and tectonic implications. Journal of Asian Earth Sciences 42, 854–866.

Gu, L.X., Hu, S.X., Yu, C.S., Zhao, M., Wu, C.Z., Li, H.Y., 2001. Intrusive activities during compression–extension tectonic conversion in the Bogda intracontinental orogen. Acta Petrologica Sinica 17, 187–198 (in Chinese with English abstract).

Han, C.M., Xiao, W.J., Zhao, G.C., Ao, S.J., Zhang, J.E., Qu, W.J., Du, A.D., 2010. In-situ U–Pb, Hf and Re–Os isotopic analyses of the Xiangshan Ni–Cu–Co deposit in Eastern Tianshan (Xinjiang), Central Asia Orogenic Belt: constraints on the timing and genesis of the mineralization. Lithos 120, 547–562.

Herzberg, C., O'Hara, M.J., 2002. Plume-associated ultramafic magmas of Phanerozoic age. Journal of Petrology 43, 1857–1883.

Hong, D.W., Wang, S.G., Xie, X.L., Zhang, J.S., 2001. The Phanerozoic continental growth in central Asia and the evolution of Laurasia supercontinent. Gondwana Research 4, 632–633.

Hu, A.Q., Jahn, B.M., Zhang, G., Chen, Y., Zhang, Q., 2000. Crustal evolution and Phanerozoic crustal growth in northern Xinjiang: Nd isotope evidence. 1. Isotopic characterization of basement rocks. Tectonophysics 328, 15–51.

Isley, A.E., Abbott, D.H., 2002. Implications of the temporal distribution of high-Mg magmas for mantle plume volcanism through time. Journal of Geology 110, 141–158.

Jahn, B.M., Wu, F.Y., Chen, B., 2000a. Massive granitoid generation in Central Asia: Nd isotope evidence and implication for continental growth in the Phanerozoic. Episodes 23, 82–92.

Jahn, B.M., Wu, F., Chen, B., 2000b. Granitoids of the Central Asian orogenic belt and continental growth in the Phanerozoic. Royal Society of Edinburgh: Earth Science 91, 181–193.

Jahn, B.M., Windley, B., Natal'in, B., Dobretsov, N., 2004. Phanerozoic continental growth in Central Asia. Journal of Asian Earth Sciences 23, 599–603.

James, D.E., 1981. The combined use of oxygen and radiogenic isotopes as indicators of crustal contamination. Annual Review of Earth and Planetary Sciences 9, 311–344.

Jiang, C.Y., Cheng, S.L., Ye, S.F., Xia, M.Z., Jiang, H.B., Dai, Y.C., 2006. Lithogeochemistry and petrogenesis of Zhongposhanbei mafic rock body, at Beishan region, Xinjiang. Acta Petrologica Sinica 22, 115–126 (in Chinese with English abstract).

Jourdan, F., Bertrand, H., Feraud, G., Le Gall, B., Watkeys, M.K., 2009. Lithospheric mantle evolution monitored by overlapping large igneous provinces: case study in southern Africa. Lithos 107, 257–268.

Li, J.Y., Song, B., Wang, K.Z., Li, Y.P., Sun, G.H., Qi, D.Y., 2006. Permian mafic–ultramafic complexes on the southern margin of the Tu–Ha Basin, east Tianshan Mountains: geological records of vertical crustal growth in central Asia. Acta Geoscientica Sinica 27, 424–446 (in Chinese with English abstract).

Li, J.Z., Wu, X.Z., Qi, X.F., Zhang, M., Zhang, Q.C., 2010. Distribution and tectonic setting of upper Paleozoic volcanic rock in northern Xinjiang. Acta Petrologica Sinica 26, 195–206 (in Chinese with English abstract).

Liu, P.P., Qin, K.Z., Su, S.G., San, J.Z., Tang, D.M., Su, B.X., Sun, H., Xiao, Q.H., 2010. Characteristics of multiphase sulfide droplets and their implications for conduit-style mineralization of Tulargen Cu–Ni deposit, eastern Tianshan, Xinjiang. Acta Petrologica Sinica 26, 523–532 (in Chinese with English abstract).

Magaritz, M., Whitford, D.J., James, D.E., 1978. Oxygen isotopes and the origin of high $^{87}Sr/^{86}Sr$ andesites. Earth and Planetary Science Letters 40, 220–230.

Mao, Q.G., 2008. Paleozoic to Early Mesozoic accretionary and collisional tectonics of the Beishan and adjacent area, northwest China. Institute of Geology and Geophysics, Chinese Academy of Sciences. Ph.D thesis (in Chinese with English abstract).

Mao, Q.G., Xiao, W.J., Han, C.M., Sun, M., Yuan, C., Yan, Z., Li, J.L., Yong, Y., Zhang, J.E., 2006. Zircon U–Pb age and geochemistry of the Baishiquan mafic–ultramafic complex in the Eastern Tianshan, Xinjiang: constraints on the closure of the Paleo-Asian ocean. Acta Petrologica Sinica 22, 153–162 (in Chinese with English abstract).

Mao, J.W., Pirajno, F., Zhang, Z.H., Chai, F.M., Wu, H., Chen, S.P., Cheng, S.L., Yang, J.M., Zhang, C.Q., 2008. A review of the Cu–Ni sulfide deposits in the Chinese Tianshan and Altay orogens (Xinjiang Autonomous Region, NW China): principal characteristics and ore-forming processes. Journal of Asian Earth Sciences 32, 184–203.

Nakajima, T., Maruyama, S., Uchiumi, S., Liou, J.G., Wang, X.Z., Xiao, X.C., Graham, S.A., 1990. Evidence for Late Proterozoic subduction from 700-Myr-old blueschists in China. Nature 346, 263–265.

Pearce, J.W., Peate, D.W., 1995. Tectonic implications of the composition of volcanic arc magmas. Annual Review of Earth and Planetary Sciences 23, 251–285.

Pirajno, F., Mao, J.W., Zhang, Z.C., Zhang, Z.H., Chai, F.M., 2008. The association of mafic–ultramafic intrusions and A-type magmatism in the Tianshan and Altay orogens, NW China: implications for geodynamic evolution and potential for the discovery of new ore deposits. Journal of Asian Earth Sciences 32, 165–183.

Qin, K.Z., Fang, T.H., Wang, S.L., 2002. Plate tectonics division, evolution and metallogenic settings in eastern Tianshan mountains, NW China. Xinjiang Geology 20, 302–308 (in Chinese with English abstract).

Qin, K.Z., Zhang, L.C., Xiao, W.J., Xu, X.W., Yan, Z., Mao, J.W., 2003. Overview of major Au, Cu, Ni and Fe deposits and metallogenic evolution of the eastern Tianshan Mountains, Northwestern China. In: Mao, J.W., Goldfarb, R.J., Seltmann, R., Wang, D.W., Xiao, W.J., Hart, C. (Eds.), Tectonic Evolution and Metallogeny of the Chinese Altay and Tianshan, London, pp. 227–249.

Qin, K.Z., Ding, K.S., Xu, Y.X., Sun, H., Xu, X.W., Tang, D.M., Mao, Q., 2007. Ore potential of protoliths and modes of Co–Ni occurrence in Tulargen and Baishiquan Cu–Ni–Co deposits, East Tianshan, Xinjiang. Mineral Deposits 26, 1–14 (in Chinese with English abstract).

Qin, K.Z., Su, B.X., Sakyi, P.A., Tang, D.M., Li, X.H., Sun, H., Xiao, Q.H., Liu, P.P., 2011. SIMS Zircon U–Pb geochronology and Sr–Nd isotopes of Ni–Cu bearing mafic–ultramafic intrusions in Eastern Tianshan and Beishan in correlation with flood basalts in Tarim Basin (NW China): constraints on a ca. 280 Ma mantle plume. American Journal of Science 311, 237–260.

Rogers, N., Macdonald, R., Fitton, J.G., George, R., Smith, M., Barreiro, B., 2000. Two mantle plumes beneath the East African rift system: Sr, Nd and Pb isotope evidence from Kenya Rift basalts. Earth and Planetary Science Letters 176, 387–400.

Rollinson, H.R., 1993. Using Geochemical Data: Evaluation, Presentation, Interpretation. Longman Geochemistry Society, London.

San, J.Z., Qin, K.Z., Tang, Z.L., Tang, D.M., Su, B.X., Sun, H., Xiao, Q.H., Liu, P.P., 2010. Precise zircon U–Pb age dating of two mafic–ultramafic complexes at Tulargen large Cu–Ni district and its geological implications. Acta Petrologica Sinica 26, 3027–3035 (in Chinese with English abstract).

Saunders, A.D., England, R.W., Reichow, M.K., White, R.V., 2005. A mantle plume origin for the Siberian traps: uplift and extension in the West Siberian Basin, Russia. Lithos 79, 407–424.

Sengör, A.M.C., Natal'in, B.A., Burtman, V.S., 1993. Evolution of the Altaid tectonic collage and Paleozoic crustal growth in Asia. Nature 364, 299–307.

Song, X.Y., Xie, W., Deng, Y.F., Crawford, A.J., Zheng, W.Q., Zhou, G.F., Deng, G., Cheng, S.L., Li, J., 2011. Slab break-off and the formation of Permian mafic–ultramafic intrusions in southern margin of Central Asian Orogenic Belt, Xinjiang, NW China. Lithos 127, 128–143.

Su, B.X., 2010. Mafic–ultramafic Complexes in Beishan Area, Xinjiang: Petrogenesis, Mineralization and Constraints on the Tectonic Evolution of the Eastern Tianshan and Beishan, and the Early Permian Mantle Plume. Institute of Geology and Geophysics, Chinese Academy of Sciences. Ph.D thesis (in Chinese with English abstract).

Su, B.X., Qin, K.Z., Sun, H., Tang, D.M., Xiao, Q.H., Cao, M.J., 2009. Petrological and mineralogical characteristics of Hongshishan mafic–ultramafic complex in Beishan area, Xinjiang: implications for assimilation and fractional crystallization. Acta Petrologica Sinica 25, 873–887 (in Chinese with English abstract).

Su, B.X., Qin, K.Z., Sun, H., Wang, H., 2010. Geochronological, petrological, mineralogical and geochemical studies of the Xuanwoling mafic–ultramafic intrusion in the Beishan area, Xinjiang. Acta Petrologica Sinica 26, 3283–3294 (in Chinese with English abstract).

Su, B.X., Qin, K.Z., Sakyi, P.A., Liu, P.P., Tang, D.M., Malaviarachchi, S.P.K., Xiao, Q.H., Sun, H., Dai, Y.C., Hu, Y., 2011a. Geochemistry and geochronology of acidic rocks in the Beishan region, NW China: petrogenesis and tectonic implications. Journal of Asian Earth Sciences 41, 31–43.

Su, B.X., Qin, K.Z., Sakyi, P.A., Li, X.H., Yang, Y.H., Sun, H., Tang, D.M., Liu, P.P., Xiao, Q.H., Malaviarachchi, S.P.K., 2011b. U–Pb ages and Hf–O isotopes of zircons from Late Paleozoic mafic–ultramafic units in southern Central Asian Orogenic Belt: tectonic implications and evidence for an Early-Permian mantle plume. Gondwana Research 20, 516–531.

Su, B.X., Qin, K.Z., Tang, D.M., Deng, G., Xiao, Q.H., Sun, H., Lu, H.F., Dai, Y.C., 2011c. Petrological features and implications for mineralization of the Poshi mafic–ultramafic intrusion in Beishan area, Xinjiang. Acta Petrologica Sinica 27, 3627–3639 (in Chinese with English abstract).

Su, B.X., Qin, K.Z., Sakyi, P.A., Tang, D.M., Liu, P.P., Malaviarachchi, S.P.K., Xiao, Q.H., Sun, H., 2012a. Geochronologic–petrochemical studies of the Hongshishan mafic–ultramafic intrusion, Beishan area, Xinjiang (NW China): petrogenesis and tectonic implications. International Geology Review 54, 270–289.

Su, B.X., Qin, K.Z., Sakyi, P.A., Malaviarachchi, S.P.K., Liu, P.P., Tang, D.M., Xiao, Q.H., Sun, H., Ma, Y.G., Mao, Q., 2012b. Occurrence of an Alaskan-type complex in the Middle Tianshan Massif, Central Asian Orogenic Belt: inferences from petrological and mineralogical studies. International Geology Review 54, 249–269.

Su, B.X., Qin, K.Z., Sun, H., Tang, D.M., Xiao, Q.H., Liu, P.P., Sakyi, P.A., 2012c. Olivine compositional mapping of mafic–ultramafic complexes in Eastern Xinjiang (NW China): implications for mineralization and tectonic dynamics. Journal of Earth Science 23, 41–53.

Sun, H., 2009. Ore-forming mechanism in conduit system and ore-bearing property evaluation for mafic-ultramafic complex in Eastern Tianshan, Xinjiang. Institute of Geology and Geophysics, Chinese Academy of Sciences. Ph.D thesis (in Chinese with English abstract).

Sun, S.S., McDonough, W.F., 1989. Chemical and isotopic systematic of oceanic basalts: implications for mantle composition and processes. In: Saunders, A.D., Norry, M.J. (Eds.), Magmatism in the Ocean Basins: Geological Society Special Publication, pp. 313–345.

Sun, H., Qin, K.Z., Xu, X.W., Li, J.X., Ding, K.S., Xu, Y.X., San, J.Z., 2007. Petrological characteristics and copper–nickel ore-forming processes of early Permian mafic–ultramafic intrusion belts in east Tianshan. Mineral Deposits 26, 98–108 (in Chinese with English abstract).

Sun, M., Yuan, C., Xiao, W.J., Long, X.P., Xia, X.P., Zhao, G.C., Lin, S.F., Wu, F.Y., Kröner, A., 2008. Zircon U–Pb and Hf isotopic study of gneissic rocks from the Chinese Altai: progressive accretionary history in the early to middle Palaeozoic. Chemical Geology 247, 352–383.

Tang, D.M., 2009. Geochemistry and enrichment regulation of PGE in the Ni-Cu sulfide deposits of mafic-ultramafic intrusions in the Eastern Tianshan. Institute of Geology and Geophysics, Chinese Academy of Sciences. Ph.D thesis (in Chinese with English abstract).

Tang, Y.J., Zhang, H.F., Ying, J.F., 2006. Asthenosphere–lithospheric mantle interaction in an extensional regime: implication from the geochemistry of Cenozoic basalts from Taihang Mountains, North China Craton. Chemical Geology 233, 309–327.

Tang, D.M., Qin, K.Z., Sun, H., Su, B.X., Xiao, Q.H., Cheng, S.L., Li, J., 2009. Zircon U–Pb age and geochemical characteristics of Tianyu intrusion, East Tianshan: constraints on source and genesis of mafic–ultramafic intrusions in East Xinjiang. Acta Petrologica Sinica 25, 817–831 (in Chinese with English abstract).

Tang, G.J., Wang, Q., Wyman, D.A., Li, Z.X., Zhao, Z.H., Jia, X.H., Jiang, Z.Q., 2010. Ridge subduction and crustal growth in the Central Asian Orogenic Belt: evidence from Late Carboniferous adakites and high-Mg diorites in the western Junggar region, northern Xinjiang (west China). Chemical Geology 277, 281–300.

Tang, D.M., Qin, K.Z., Li, C.S., Qi, L., Su, B.X., Qu, W.J., 2011. Zircon dating, Hf–Sr–Nd–Os isotopes and PGE geochemistry of the Tianyu sulfide-bearing mafic–ultramafic intrusion in the Central Asian Orogenic Belt, NW China. Lithos 126, 84–98.

Tang, G.J., Wang, Q., Wyman, D.A., Li, Z.X., Xu, Y.G., Zhao, Z.H., 2012. Recycling oceanic crust for continental crustal growth: Sr–Nd–Hf isotope evidence from granitoids in the western Junggar region, NW China. Lithos 128, 73–83.

Turner, S., Hawkesworth, C., Rogers, N., Bartlett, J., Worthington, T., Hergt, J., Pearce, J., Smith, I., 1997. ^{238}U–^{230}Th disequilibrium, magma petrogenesis, and flux rates beneath the depleted Tonga–Kermadec island arc. Geochimica et Cosmochimica Acta 61, 4855–4884.

Valley, J.W., Kinny, P.D., Schulze, D.J., Spicuzza, M.J., 1998. Zircon megacrysts from kimberlite: oxygen isotope variability among mantle melts. Contributions to Mineralogy and Petrology 133, 1–11.

Wang, C.Y., Zhou, M.F., 2006. Genesis of the Permian Baimazhai magmatic Ni–Cu–(PGE) sulfide deposit, Yunnan, SW China. Mineralium Deposita 41, 771–783.

Wang, J.B., Wang, Y.W., He, Z.J., 2006. Ore deposits as a guide to the tectonic evolution in the East Tianshan mountains, NW China. Geology in China 33, 461–469.

Wang, T., Jahn, B.M., Kovach, V.P., Tong, Y., Hong, D.W., Han, B.F., 2009a. Nd–Sr isotopic mapping of the Chinese Altai and implications for continental growth in the Central Asian Orogenic Belt. Lithos 110, 359–372.

Wang, Y.W., Wang, J.B., Wang, L.J., Long, L.L., 2009b. Characteristics of two mafic–ultramafic rock series in the Xiangshan Cu–Ni–(V)Ti–Fe ore district, Xinjiang. Acta Petrologica Sinica 25, 888–900 (in Chinese with English abstract).

Wang, C.Y., Campbell, I.H., Allen, C.M., Williams, I.S., Eggins, S.M., 2009c. Rate of growth of the preserved North American continental crust: evidence from Hf and O isotopes in Mississippi detrital zircons. Geochimica et Cosmochimica Acta 73, 712–728.

Windley, B.F., Alexeiev, D., Xiao, W., Kroner, A., Badarch, G., 2007. Tectonic models for accretion of the Central Asian Orogenic Belt. Journal of the Geological Society of London 164, 31–47.

Xia, M.Z., Jiang, C.Y., Qian, Z.Z., Xia, Z.D., Lu, R.H., 2008. Geochemistry and petrogenesis for Hulu intrusion in East Tianshan, Xinjiang. Acta Petrologica Sinica 24, 2749–2760 (in Chinese with English abstract).

Xiao, W.J., Windley, B.F., Hao, J., Zhai, M.G., 2003. Accretion leading to collision and the Permian Solonker suture, Inner Mongolia, China: termination of the central Asian orogenic belt. Tectonics 22, 1069.

Xiao, W.J., Zhang, L.C., Qin, K.Z., Sun, S., Li, J.L., 2004a. Paleozoic accretionary and collisional tectonics of the eastern Tianshan (China): implications for the continental growth of Central Asia. American Journal of Science 304, 370–395.

Xiao, L., Xu, Y.G., Mei, H.J., Zheng, Y.F., He, B., Pirajno, F., 2004b. Distinct mantle sources of low-Ti and high-Ti basalts from the western Emeishan large igneous province, SW China: implications for plume–lithosphere interaction. Earth and Planetary Science Letters 228, 525–546.

Xiao, W.J., Windley, B.F., Yuan, C., Sun, M., Han, C.M., Lin, S.F., Chen, H.L., Yan, Q.R., Liu, D.Y., Qin, K.Z., Li, J.L., Sun, S., 2009. Paleozoic multiple subduction–accretion processes of the southern Altaids. American Journal of Science 309, 221–270.

Xiao, Q.H., Qin, K.Z., Tang, D.M., Su, B.X., Sun, H., San, J.Z., Cao, M.J., Hui, W.D., 2010. Xiangshan composite Cu–Ni–Ti–Fe and Ni–Cu deposit belongs to comagmatic evolution product: evidence from ore microscopy, zircon U–Pb chronology and petrological geochemistry, Hami, Xinjiang, NW China. Acta Petrologica Sinica 26, 503–522 (in Chinese with English abstract).

Xiao, Y., Zhang, H.F., Shi, J.A., Su, B.X., Sakyi, P.A., Hu, Y., Zhang, Z., 2011. Late Paleozoic magmatic record of East Junggar, NW China and its significance: implication from zircon U–Pb dating and Hf isotope. Gondwana Research 20, 532–542.

Xu, Y.G., Chung, S.L., Jahn, B.M., Wu, G.Y., 2001. Petrologic and geochemical constraints on the petrogenesis of Permian–Triassic Emeishan flood basalts in southwestern China. Lithos 58, 145–168.

Xu, X.Y., He, S.P., Wang, H.L., Chen, J.L., 2009. Geological Background Map of Mineralization in Eastern Tianshan–Beishan Area. (in Chinese).

Yue, Y.J., Liou, J.G., Graham, S.A., 2001. Tectonic correlation of Beishan and Inner Mongolia orogens and its implications for the palinspastic reconstruction of north China. In: Hendrix, M.S., Davis, G.A. (Eds.), Paleozoic and Mesozoic tectonic evolution of central Asia. : From continental assembly to intracontinental deformation, 194. Geological Society of America Memoir, Boulder, Colorado, pp. 101–116.

Zhang, H.F., Sun, M., Lu, F.X., Zhou, X.H., Zhou, M.F., Liu, Y.S., Zhang, G.H., 2001. Geochemical significance of a garnet lherzolite from the Dahongshan kimberlite, Yangtze Craton, southern China. Geochemical Journal 35, 315–331.

Zhang, L.F., Ellis, D.J., Jiang, W., 2002. Ultrahigh pressure metamorphism in western Tianshan, China, part I: evidences from the inclusion of coesite pseudomorphs in garnet and quartz exsolution lamellae in omphacite in eclogites. American Mineralogist 87, 853–860.

Zhang, L.C., Qin, K.Z., Ying, J.F., Xia, B., Shu, J.S., 2004. The relationship between ore-forming processes and adakitic rock in Tuwu-Yandong porphyry copper metallogenic belt, eastern Tianshan mountains. Acta Petrologica Sinica 20, 259–268 (in Chinese with English abstract).

Zhang, Z.Z., Gu, L.X., Wu, C.Z., Zhai, J.P., Li, W.Q., Tang, J.H., 2007. Early Indosinian Weiya Gabbro in Eastern Tianshan, China: elemental and Sr–Nd–O isotopic geochemistry, and its tectonic implications. Acta Geologica Sinica 81, 424–432.

Zhang, C.L., Li, X.H., Li, Z.X., Ye, H.M., Li, C.N., 2008. A Permian layered intrusive complex in the Western Tarim Block, northwestern China: product of a ca. 275-Ma mantle plume? Journal of Geology 116, 269–287.

Zhang, Z.C., Mao, J.W., Chai, F.M., Yan, S.H., Chen, B.L., Pirajno, F., 2009. Geochemistry of the Permian Kalatongke mafic intrusions, northern Xinjiang, northwest China: implications for the genesis of magmatic Ni–Cu sulfide deposits. Economic Geology 104, 185–203.

Zhao, J.H., Zhou, M.F., 2007. Geochemistry of Neoproterozoic mafic intrusions in the Panzhihua district (Sichuan Province, SW China): implications for subduction-related metasomatism in the upper mantle. Precambrian Research 152, 27–47.

Zhao, D.P., Lei, J.S., Inoue, T., Yamada, A., Gao, S.S., 2006. Deep structure and origin of the Baikal rift zone. Earth and Planetary Science Letters 243, 681–691.

Zhou, M.F., Lesher, C.M., Yang, Z.X., Li, J.W., Sun, M., 2004. Geochemistry and petrogenesis of 270 Ma Ni–Cu–(PGE) sulfide-bearing mafic intrusions in the Huangshan district, Eastern Xinjiang, Northwest China: implications for the tectonic evolution of the Central Asian Orogenic Belt. Chemical Geology 209, 233–257.

Zhou, T.F., Yuan, F., Fan, Y., Zhang, D.Y., Cooke, D., Zhao, G.C., 2008. Granites in the Sawuer region of the west Junggar, Xinjiang Province, China: geochronological and geochemical characteristics and their geodynamic significance. Lithos 106, 191–206.

Zhou, M.F., Zhao, J.H., Jiang, C.Y., Gao, J.F., Wang, W., Yang, S.H., 2009. OIB-like, heterogeneous mantle sources of Permian basaltic magmatism in the western Tarim Basin, NW China: implications for a possible Permian large igneous province. Lithos 113, 583–594.

Zindler, A., Hart, S.R., 1986. Chemical geodynamics. Annual Review of Earth and Planetary Sciences 14, 493–571.